

Supporting Information

A critical study of the generality of the two step two electron pathway for water splitting by application of a C_3N_4/MnO_2 photocatalyst

Juan Liu,^{‡a} Naiyun Liu,^{‡a} Hao Li,^a Liping Wang,^a Xiuqin Wu,^a Hui Huang,^a Yang Liu,^{*a} Feng Bao,^a Yeshayahu Lifshitz,^{*b} Shuit-Tong Lee^a and Zhenhui Kang^{*a}

^a *Jiangsu Key Laboratory for Carbon-based Functional Materials and Devices, Institute of Functional Nano and Soft Materials (FUNSOM), Soochow University, Suzhou, Jiangsu 215123, China. E-mail: zhkang@suda.edu.cn; yangl@suda.edu.cn*

^b *Department of Materials Science and Engineering, Technion, Israel Institute of Technology, Haifa 32000, Israel. E-mail: shayli@technion.ac.il*

[‡]These two authors are equally main contributors.

1 Experimental Section

Preparation of C_3N_4 . Carbon nitride (C_3N_4) was synthesized following previous reports.^[3] 10 g of urea powder was put into an alumina crucible with a cover and then heated to 550 °C with a heating rate of 5 °C/min in a muffle furnace and maintained at this temperature for 3 h. The light yellow powder obtained after cooling was C_3N_4 .

Preparation of C_3N_4/MnO_2 Photocatalysts. $KMnO_4$ (0.63 mmol, 0.1 g) and 0.6 g C_3N_4 (obtained by heating urea at 550°C for 3 hours) were added into 500 mL ultrapure water, and stirred for 12 h. After centrifuging for 3 times to remove the excess $KMnO_4$, 10 mL oleinic acid was added into the turbid liquid. Stirring it again for 24 h. The resulting product was centrifuged and washed with acetone, ethyl and water many times till all the oleinic acid was removed. The product is then dried at 60 °C in an oven till it becomes a powder. The weight of the final product is 0.6066 g.

Photocatalyst Characterization. The crystalline structure of the resultant products was characterized by X-ray powder diffraction (XRD) by using a X'Pert-ProMPD (Holand) D/max- γ AX-ray diffractometer with Cu K α radiation ($\lambda=0.154178$ nm). Transmission electron microscopy (TEM), high-resolution TEM (HRTEM) images and EELS spectra were obtained with a FEI/Philips Tecnai 12 BioTWIN transmission electron microscope and a CM200 FEG transmission electron microscope, respectively. The TEM samples were prepared by dropping the solution onto a copper grid with carbon support film and dried in air, respectively. Room temperature UV-Vis absorption was recorded on a Lambda 750 (Perking Elmer) spectrophotometer in the wavelength range of 300–800 nm. The Fourier transform infrared (FTIR) spectrum was recorded on a FTIR spectrometer (Spectrum One, Perkin Elmer) using a standard KBr pellet technique. X-ray photoelectron spectroscopy (XPS) was obtained by using a KRATOS Axis ultra-DLD X-ray photoelectron spectrometer with a monochromatised Mg K α X-ray ($h\nu = 1283.3$ eV). Ultraviolet photoelectron spectroscopy (UPS) measurements are performed with an unfiltered HeI (21.22 eV) gas discharge lamp and a total instrumental energy resolution of 100 meV.

Photocatalysis activity tests. The photocatalytic reactions of the composite photocatalysts were carried out in an outer irradiation-type photoreactor (Pyrex glass) connected to a closed gas-circulation system. Approximately 0.100 g photocatalysts were dispersed by a magnetic stirrer in 100 mL ultrapure water. The suspension was thoroughly degassed to remove air and irradiated using a 300 W Xe-lamp (PLS-SXE 300, Beijing Trusttech Co. Ltd, China). A cutoff filter (Kenko L-42) was employed for the visible light ($\lambda>420$ nm) irradiation and band-pass filters were used for measurements of the hydrogen generation quantum efficiency. The power density measured for the $\lambda>420$ nm irradiation was 18.4 mW/cm² and for the band-pass filters one order of magnitude lower. The photocatalytic gas evolution rate was analyzed using an online SP-6890 gas chromatograph (TCD detector, 5 A° molecular sieve columns and N₂ carrier). The first four 24 h experiments were done with Ar as a carrier gas and no N₂ was detected ruling out air leaking or corrosion of the C₃N₄ catalyst releasing N₂.

Electrochemical measurements. The hydrogen peroxide generation tests were performed using a rotating ring-disk electrode (RRDE) at a scan rate of 10 mV/s. A platinum wire was the auxiliary electrode and a saturated calomel electrode (SCE, saturated KCl) was the reference electrode. The working electrodes were prepared by spreading 10 μ L 0.1 g/L catalysts dispersed in ethanol on a Pt disk (3.0 mm in diameter)-Pt ring RRDE system (Jiangsu Jiangfen Electroanalytical Instrument Co. Ltd.). The I-V curves of the electrodes were tested in a conventional three-electrode electrochemical cell with a platinum wire as the auxiliary electrode and a SCE as the reference electrode. The working electrode is 10 μ L 0.1 g/L C₃N₄/MnO₂ dripped on glassy carbon electrode in 100 mL ultrapure water solution at a scan rate of 20 mV/s. The current signal was recorded with a CHI 660C workstation (CH Instruments, Chenhua, Shanghai, China). All electrochemical experiments were carried out at room temperature.

2 Quantum efficiency calculation.

The apparent quantum efficiency (QE) for H₂ evolution is measured using a 420 nm band-pass filter. The wavelength is from 400 nm to 440 nm. The average intensity of irradiation is determined to be 2.84 mW·cm⁻² by ILT 950 spectroradiometer (International Light Technologies) and the irradiation area is controlled as 4.52 cm². The number of incident photons (N) is 2.34×10²¹ calculated by Equation S1. The produced H₂ molecules quantity is 74.4 μ mol in 24 h (Fig. S18). The amount of H₂ gas produced in the subsequent 24 h is used to calculate quantum efficiency according to the Equation S2 shown below.

$$N = \frac{E\lambda}{hc} = \frac{2.84 \times 10^{-3} \times 4.52 \times 24 \times 3600 \times 420 \times 10^{-9}}{6.626 \times 10^{-34} \times 3 \times 10^8} = 2.34 \times 10^{21} \quad \text{Equation S1}$$

So,

$$\begin{aligned}
 \text{QE} &= \frac{2 \times \text{the number of evolved H}_2 \text{ molecules}}{\text{the number of incident photons}} \times 100\% \\
 &= \frac{2 \times 74.4 \times 10^{-6} \times 6.02 \times 10^{23}}{2.34 \times 10^{21}} \times 100\% = 3.82\% \quad \text{Equation S2}
 \end{aligned}$$

3 Electron-transfer number (n) calculation.

The electron-transfer number (n) is calculated as follows:

$$n = \frac{4I_{\text{disk}}}{I_{\text{disk}} + I_{\text{ring}} / N} \quad \text{Equation S3}$$

Here N is the RRDE collection efficiency, determined to be 0.24. Reversible system $[\text{Fe}(\text{CN})_6]^{4-}/[\text{Fe}(\text{CN})_6]^{3-}$ is used for RRDE electrode collection efficiency measurement. In details, The RRDE electrode is dipped into 0.01 mol/L $\text{K}_3[\text{Fe}(\text{CN})_6]$ in 0.1 mol/L KCl solution and rotated under different rotation rates ($\omega = 100, 400, 900, 1600, 2500$ rpm). Disk potential E_D is scanned from 0.35 V to -0.55 V vs. SCE at scan rate 10 mV/s, ring potential E_R is fixed to 0.497 V vs. SCE (the reduced product $[\text{Fe}(\text{CN})_6]^{4-}$ can be oxidized at this potential), and the current-potential voltammograms are recorded during the electrode rotation. Fig. S15 shows the RRDE measurement. The ratio of $I_{\text{ring}}/I_{\text{disk}}$ is almost constant under various ω . The average of collection efficiency N is 0.24.

4 The whole photocatalysis water splitting process on $\text{MnO}_2/\text{C}_3\text{N}_4$.

The whole photocatalysis water splitting process on $\text{MnO}_2/\text{C}_3\text{N}_4$ includes four reactions as follow:

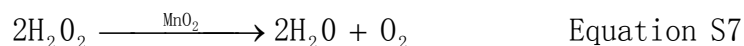
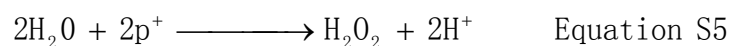


Table S1 Photocatalytic activities of different loading ratios of C₃N₄/MnO₂ for water splitting under visible light irradiation ($\lambda > 420$ nm) for 24 h. The incident light intensity is fixed at 18.4 mW cm⁻². The QE for H₂ evolution is measured using 300 W Xe lamp with a 420 nm band-pass filter. The catalyst concentration is 1 g/L.

MnO₂: C₃N₄ (mass ratio, g/g)	H₂ (O₂) evolution amount* (μmol)	QE* at 420 nm (%)
0.011	15.6 (7.7)	0.24
0.054	81.4 (40.8)	2.17
0.136	132.8 (66.5)	3.82
0.528	116.7 (58.4)	3.32
0.973	112.1 (56.0)	2.96
2.049	75.2 (37.4)	1.83
5.155	27.2 (13.5)	0.65

* These data are the average results based on three parallel experiments.

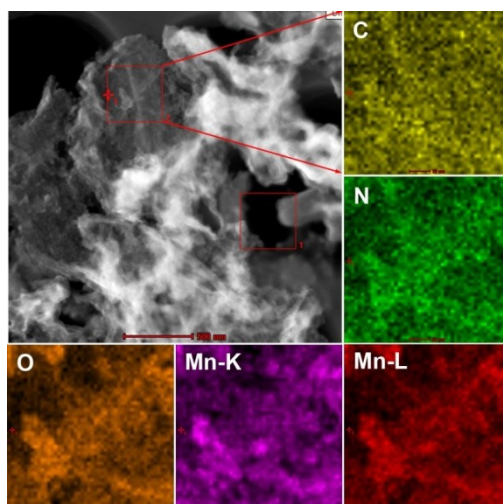


Fig. S1 The mapping patterns for the C_3N_4/MnO_2 , with a MnO_2 concentration of $0.136 \text{ g}_{MnO_2}/\text{g}_{C_3N_4}$.

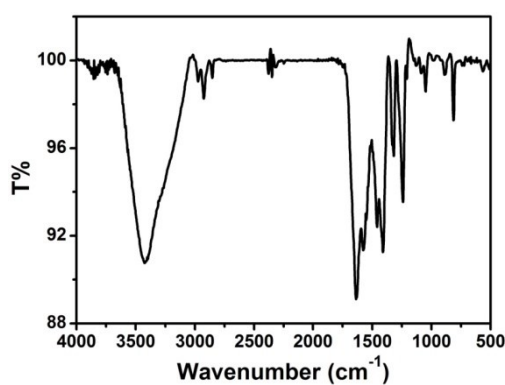


Fig. S2 The FT-IR spectra of C_3N_4/MnO_2 (the MnO_2 concentration of $0.136 \text{ g}_{MnO_2}/\text{g}_{C_3N_4}$). The spectra present several major bands between 1200 cm^{-1} and 1650 cm^{-1} region, which correspond to the characteristic stretching modes of CN heterocycles. In addition, the breathing mode of triazine units at 809 cm^{-1} is observed.

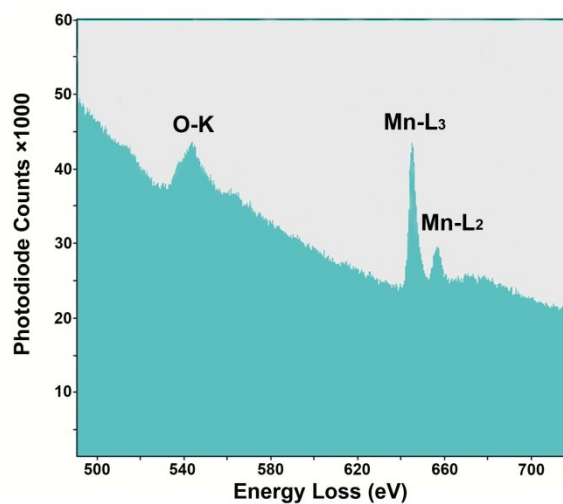


Fig. S3 Electron energy loss spectroscopy (EELS) spectra of C_3N_4/MnO_2 (the MnO_2 concentration of $5.155 \text{ g}_{MnO_2}/\text{g}_{C_3N_4}$).

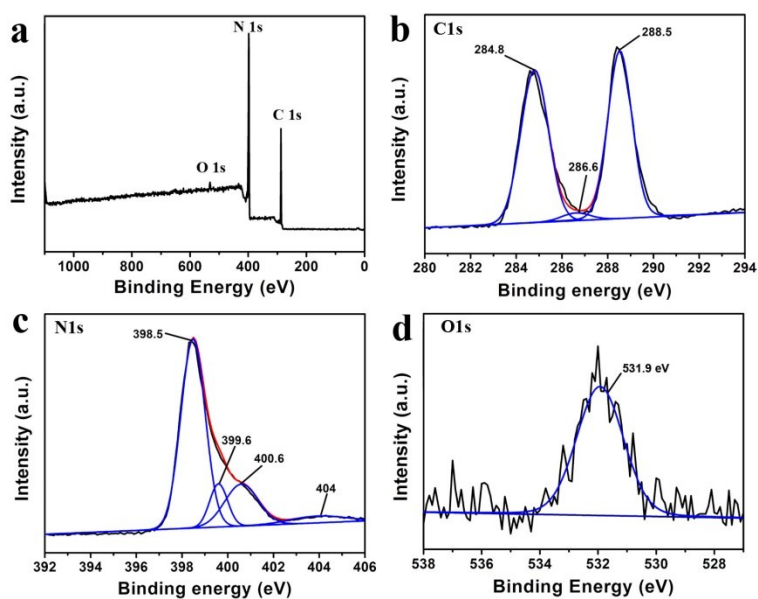


Fig. S4 XPS spectra of C_3N_4 prepared by pyrolysis of urea at $550 \text{ }^\circ\text{C}$. (a) XPS survey spectrum. (b) C1s spectrum. (c) N1s spectrum. (d) O1s spectrum.

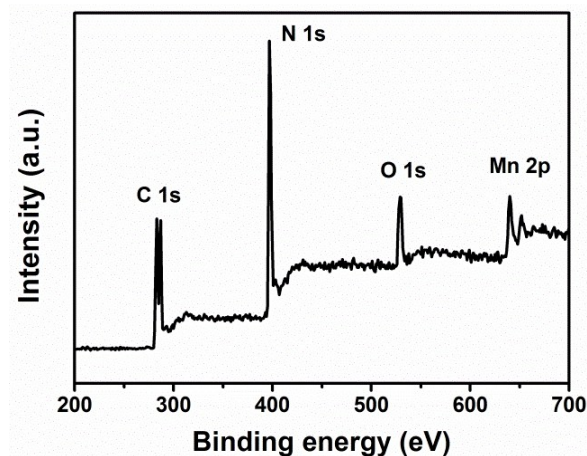


Fig. S5 The XPS survey spectra of the C_3N_4/MnO_2 (the MnO_2 concentration of 0.136 $g_{MnO_2}/g_{C_3N_4}$).

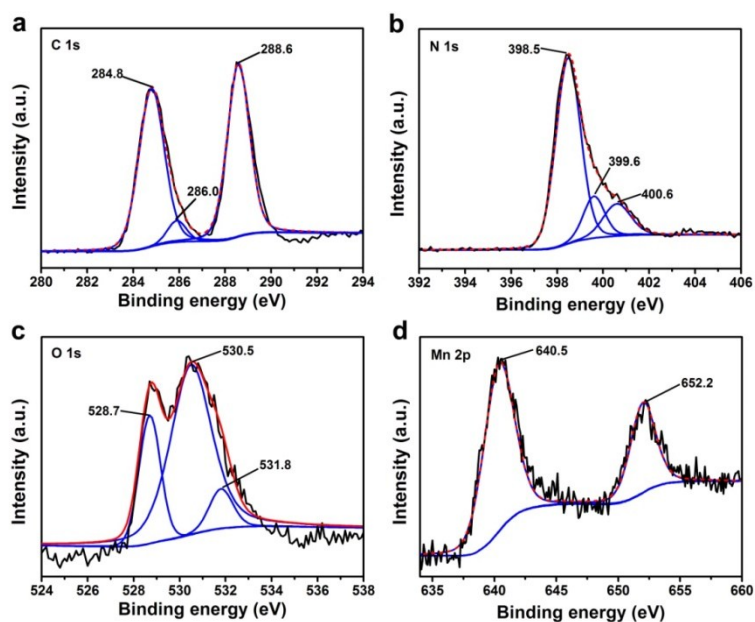


Fig. S6 The XPS spectra of the C_3N_4/MnO_2 . (a) C 1s spectra. (b) N 1s spectra. (c) O 1s spectra. (d) Mn 2P spectra.

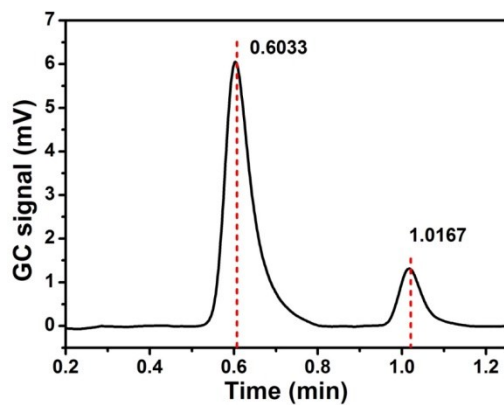


Fig. S7 A typical gas chromatograph trace of evolved hydrogen and oxygen. The gas chromatograph signal peaks at 0.6033 and 1.0167 min are attributed to H₂ and O₂ evolution respectively with a true intensity ratio of 2:1.

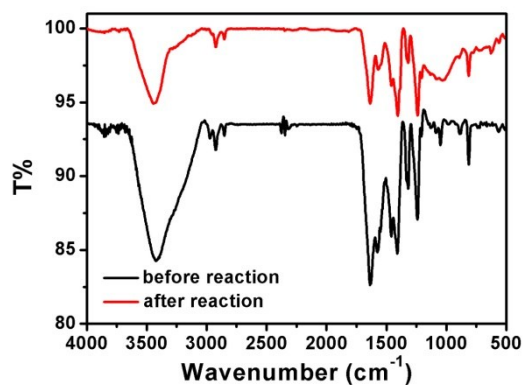


Fig. S8 FT-IR spectra of C₃N₄/MnO₂ ($g_{\text{MnO}_2}/g_{\text{C}_3\text{N}_4}=0.1$) powders after 100 cycles of 24 h water splitting.

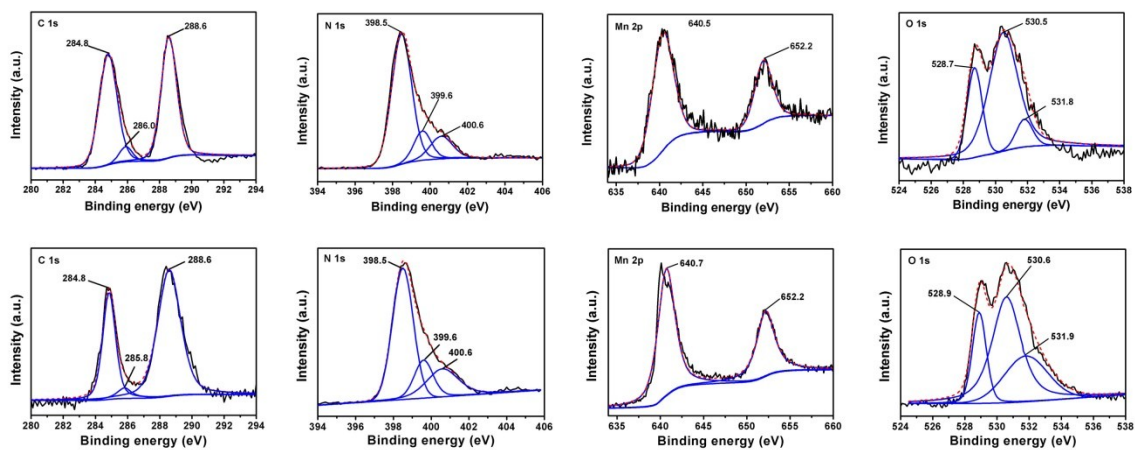


Fig. S9 XPS spectra of C_3N_4/MnO_2 ($g_{MnO_2}/g_{C_3N_4}=0.1$) before (a-c) and after (d-f) 100 cycles of 24 h water splitting. (a, d) C1s spectrum. (b, e) N1s spectrum. (c, f) Mn 2p spectrum. (d,g) O1s spectrum.

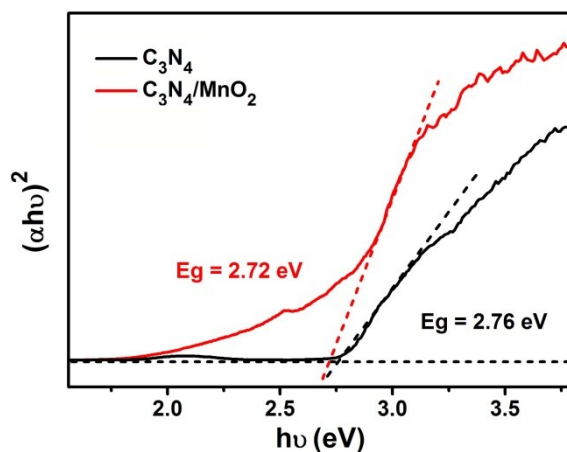


Fig. S10 Tauc plots $((\alpha h\nu)^2$ vs. $h\nu$ curves) of C_3N_4 (black trace) and C_3N_4/MnO_2 (red trace). The MnO_2 loading was $0.136 g_{MnO_2}/g_{C_3N_4}$.

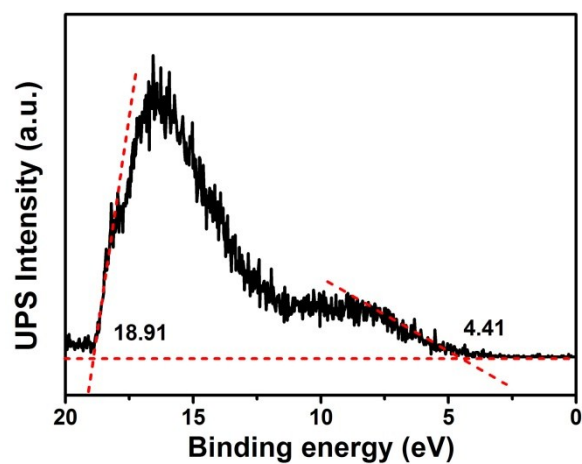


Fig. S11 The UPS spectra of the C_3N_4/MnO_2 . The MnO_2 loading was 0.136 $g_{MnO_2}/g_{C_3N_4}$.

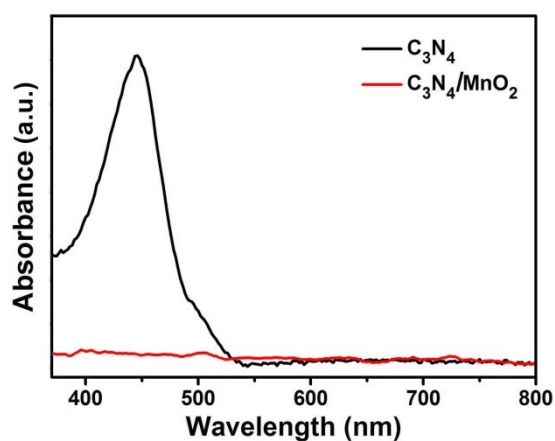


Fig. S12 The H_2O_2 amount in the reaction solution after visible light irradiation (300 W Xe lamp with a cutoff filter to acquire $\lambda > 420$ nm, the intensity is 18.4 mW cm^{-2}) for 12 h. The reaction system is 100 mg catalyst dispersed in 100 mL water. (black trace) C_3N_4 as catalyst, (red trace) C_3N_4/MnO_2 as catalyst (the MnO_2 loading was $0.136 \text{ g}_{MnO_2}/\text{g}_{C_3N_4}$).

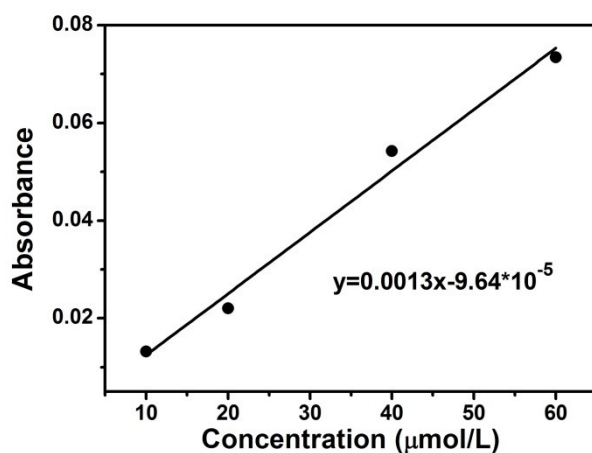


Fig. S13 The calibration curve and the fitting equation of the H_2O_2 concentration versus 446 nm absorbance, which are determined by measuring known concentrations of H_2O_2 .

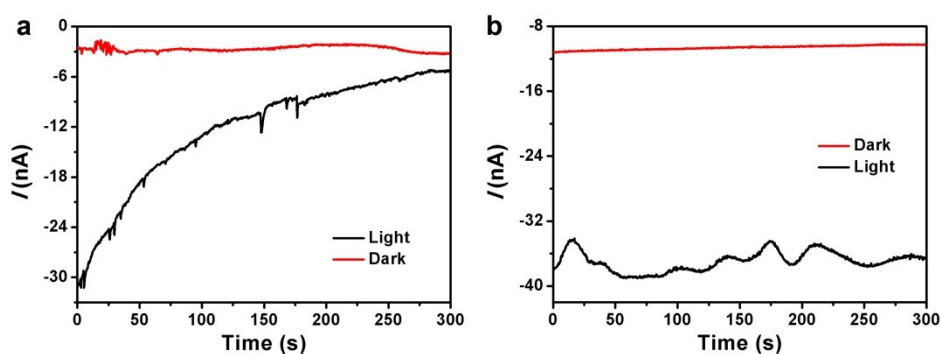


Fig. S14 The current-time curve of (a) C_3N_4 and (b) $\text{C}_3\text{N}_4/\text{MnO}_2$ ($g_{\text{MnO}_2}/g_{\text{C}_3\text{N}_4}=0.136$). The photocurrents were measured at a bias which nulls the current under dark conditions in ultrapure water solution under 300 W Xe lamp with a $\lambda > 420$ nm cut-off filter. The light intensity is 18.4 mW cm^{-2} . The C_3N_4 curve (black trace in a) shows a rapid decrease of the photocurrent indicating poisoning of the catalyst surface by H_2O_2 . The $\text{C}_3\text{N}_4/\text{MnO}_2$ curve (black trace in b) shows current oscillations between 33.5-38 nA due to cycles of H_2O_2 generation, adsorption, decomposition by MnO_2 and diffusion.

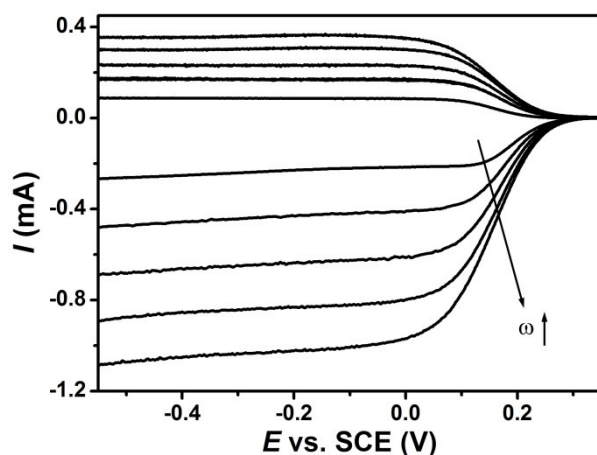


Fig. S15 I-V curves of bare RRDE in 0.1 M KCl containing 0.01 M $\text{K}_3\text{Fe}(\text{CN})_6$ under rotation rates: 100, 400, 900, 1600 and 2500 rpm (from inner to outer).

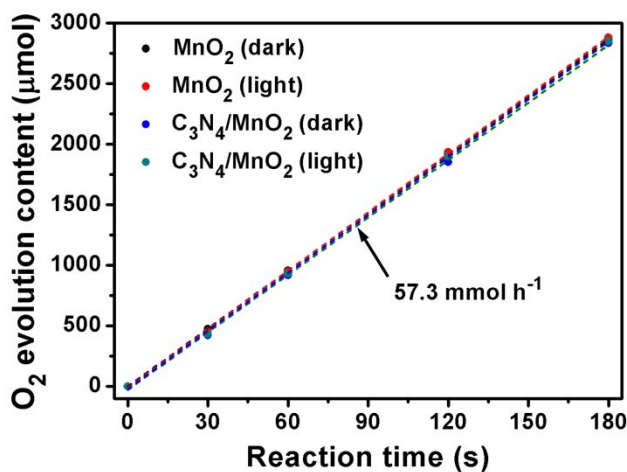


Fig. S16 O_2 evolution rate from hydrogen peroxide decomposition catalyzed by $\text{C}_3\text{N}_4/\text{MnO}_2$ ($0.136 \text{ g}_{\text{MnO}_2}/\text{g}_{\text{C}_3\text{N}_4}$) or MnO_2 as a function of reaction time under either dark or light irradiation. Reaction conditions: 100 mg of $\text{C}_3\text{N}_4/\text{MnO}_2$ or 0.01 g MnO_2 and 100 ml 0.5 M N_2 -saturation H_2O_2 aqueous solution; light source: 300 W Xe-lamp fitted with a cutoff filter (L-42) to remove light of $\lambda < 420 \text{ nm}$.

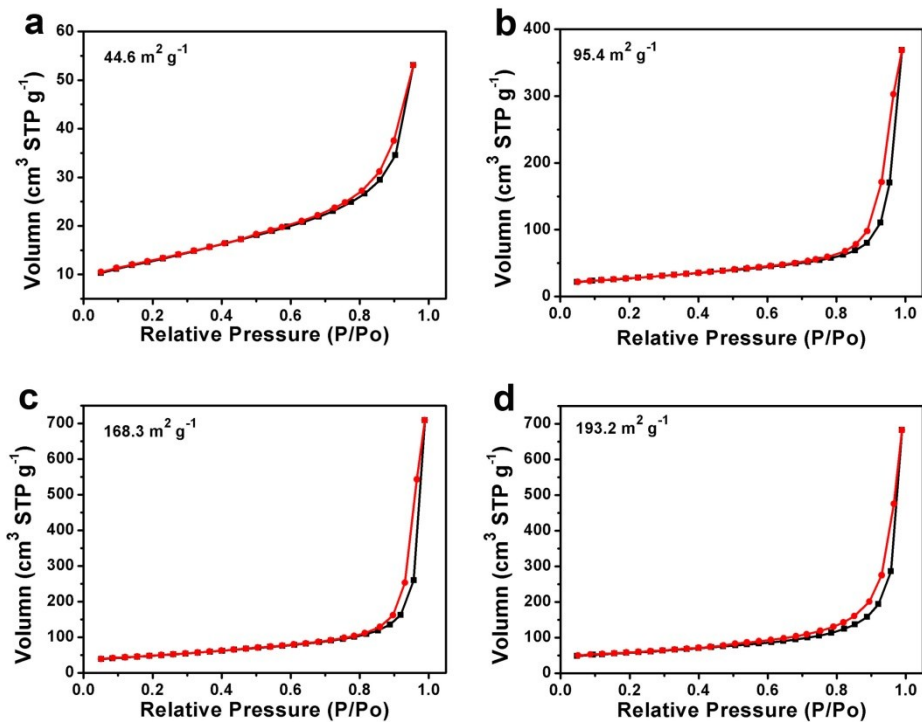


Fig. S17 N₂ adsorption and desorption isotherms at 78 K. BET surface area was measured by Tristar II 3020.

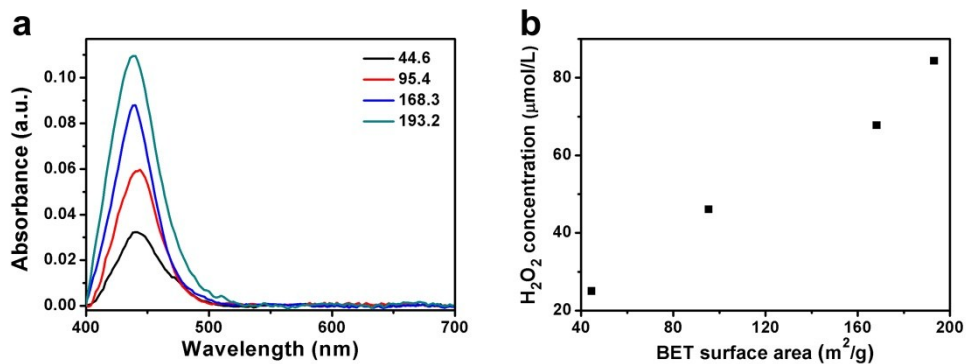


Fig. S18 (a) The H₂O₂ amount in the reaction solution after irradiation for 12 h. The reaction system is 100 mg catalyst dispersed in 100 ml water. (black trace) C₃N₄-44.6 as catalyst, (red trace) C₃N₄-95.4 as catalyst, (blue trace) C₃N₄-168.3 as catalyst, (red trace) C₃N₄-193.2 as catalyst. (b) H₂O₂ evolution for C₃N₄ with different internal surface area in the composite catalyst from the average value of BET test.

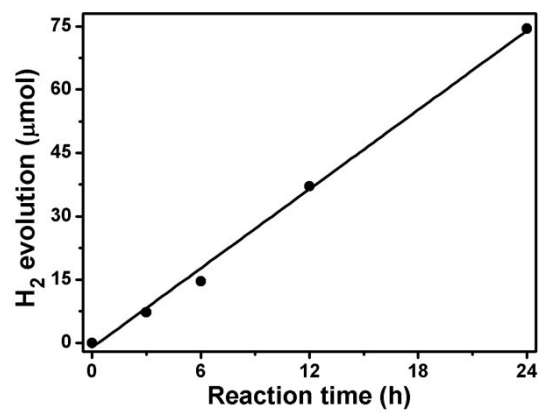


Fig. S19 The H₂ evolution curve used for determination of QE (420 ± 20 nm). A 300 W Xe lamp with a bandpass filter were used.